Supplemental Information

Supplemental experimental procedures

Fructose and glucose uptake analysis of *in vitro* studies

Lung cancer (LC) cell lines were cultured in glucose-free DMEM with 10% dialyzed fetal bovine serum (dFBS) and distinct concentrations of glucose. Spent media were collected for fructose uptake examination under distinct glucose conditions. Additionally, we investigated the impact of *SLC2A5* ablation or GLUT5 overexpression on fructose uptake and glucose uptake of LC cell lines. The commercial kits, fructose colorimetric/fluorometric assay kit (Sigma) and glucose (HK) assay kit (Sigma), were used following the manufacturer's protocol.

Cell proliferation, cell viability, cell apoptosis and cell colony formation

Cells were cultured in medium prepared with glucose-free DMEM,10% dFBS and sugar(s) indicated in figures or figure legends. Cell proliferation and cell viability were analyzed using a Cell Counting Kit-8 (CCK-8, Dojindo Laboratories) according to the manufacturer's recommendation. Cell apoptosis was measured using a FITC Annexin V Apoptosis Detection Kit (BD) following the manufacturer's protocol.

Immunohistochemistry (IHC) staining and histologic evaluation

Paired adjacent normal lung tissues and tumorous lung tissues of LC patients with adenocarcinoma (ADC) or squamous cell carcinoma (SCC) were harvested to construct tissue microarray according to previous description (1). Tissue microarray was stained with antibody against GLUT5, Ki67, CyclinD1, cleaved-Caspase 3, CD31 or nonspecific IgG as a negative control. The tissue sections were quantitatively scored based on the percentage of positive cells and staining intensity as described previously (2). The mean percentage of positive cells were computed in five areas of a given sample at a magnification of × 400 and scored from 0 – 100%. The staining intensity was scored as 0 for negative, 1 for weak, 2 for moderate, and 3 for strong. The proportion and intensity scores were then combined to obtain a weighted staining score for each case, ranging from 0 (0% of cells stained) to 3

(100% of cells stained). We defined the score < 1.5 as low GLUT5 staining and > 1.5 as high GLUT5 staining.

Serum alanine transaminase (ALT) and aspartate transaminase (AST) measurement

We measured the concentrations of serum alanine transaminase (ALT) and aspartate transaminase (AST) using ALT and AST assay kits (Nanjing Jiancheng Bioengineering Institute). The substrate was mixed with standards and samples respectively. The mixture was incubated at 37℃ for 30 minutes. Then DNPH was added to terminate the reaction. Rufous product, which was linearly correlated to ALT and AST levels, would be generated after adding NaOH. The signal of rufous product was recorded with the absorbance at 505 nm. The concentrations of ALT and AST were then determined by the standard curve.

Analysis of the public TCGA RNA-Seq and microarray datasets

TCGA datasets and GEO datasets including GSE10072 and GSE75037 were downloaded from The Cancer Genome Atlas (https://cancergenome.nih.gov/) and the NCBI Gene Expression Omnibus (http://www.ncbi.nlm.nih.gov/geo/) respectively. TCGA dataset were normalized using FPKM-UQ algorithm. FPKM method was to normalize an expression value by taking into account each protein-coding gene length and the number of reads mappable to all protein-coding genes. FPKM-UQ method was to normalize raw read count in which gene expression values, in FPKM, by dividing the 75th percentile value. GSE10072 dataset was normalized using Robust Multichip Average method 5. GSE75037 dataset was processed with the MBCB algorithm which is a background-correction and summarization method, then quantile-normalized and $\log_2$-transformed.

Supplementary references:

1. Li, X., et al. 2016. A splicing switch from ketohexokinase-C to ketohexokinase-A drives hepatocellular carcinoma formation. *Nat Cell Biol* 18:561-571.
2. Yu, G., et al. 2015. PKM2 regulates neural invasion of and predicts poor prognosis for human hilar cholangiocarcinoma. *Mol Cancer* 14:193.

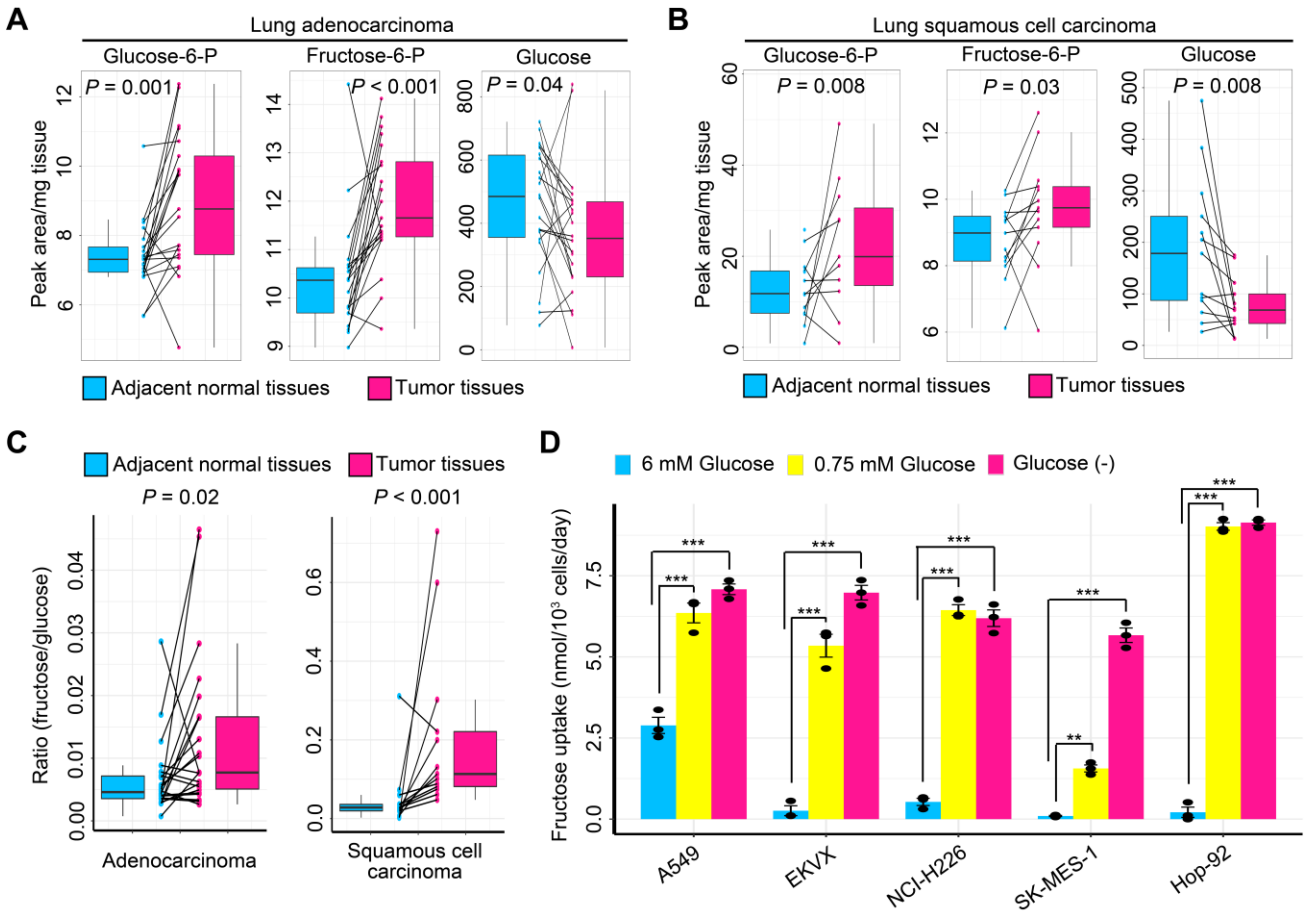

Supplemental Figure 1. High glycolytic activity in lung cancer tissues of patients and increased fructose uptake by lung cancer cells under glucose-limiting conditions. (**A** and **B**) Concentrations of glycolytic metabolites and glucose between paired adjacent normal lung tissues and tumor tissues from patients with lung adenocarcinoma (n = 22) (**A**) or lung squamous cell carcinoma (n = 13) (**B**). Glucose-6-P, glucose-6-phophate; Fructose-6-P, fructose-6-phophate. The midline represented the median of the data, with the upper and lower limits of the box being the third and first quartile. Additionally, the whiskers of the boxplot extended up to 1.5 times of the interquartile range from the top or bottom of the box. *P* values were computed using 2-tailed Wilcoxon rank-sum test. (**C**) Ratio of fructose and glucose between paired adjacent normal lung tissues and tumor tissues from patients with lung adenocarcinoma (n = 22) or lung squamous cell carcinoma (n = 13). The midline represented the median of the data, with the upper and lower limits of the box being the third and first quartile. Additionally, the whiskers of the boxplot extended up to 1.5 times of the interquartile range from the top or bottom of the box. *P* values were computed using 2-tailed Wilcoxon rank-sum test. (**D**) Fructose uptake by LC cells under conditions of distinct

glucose levels. Statistical analysis was conducted using one-way ANOVA test. For each cell line, after carrying out homogeneity of variance test to confirm equal variance among subgroups, *P* values were acquired from Post Hoc test using LSD algorism. Cumulative data are shown; n = 3. Error bars represent mean ± SEM. *** $P < 0.001$, 2-tailed Student's t test.

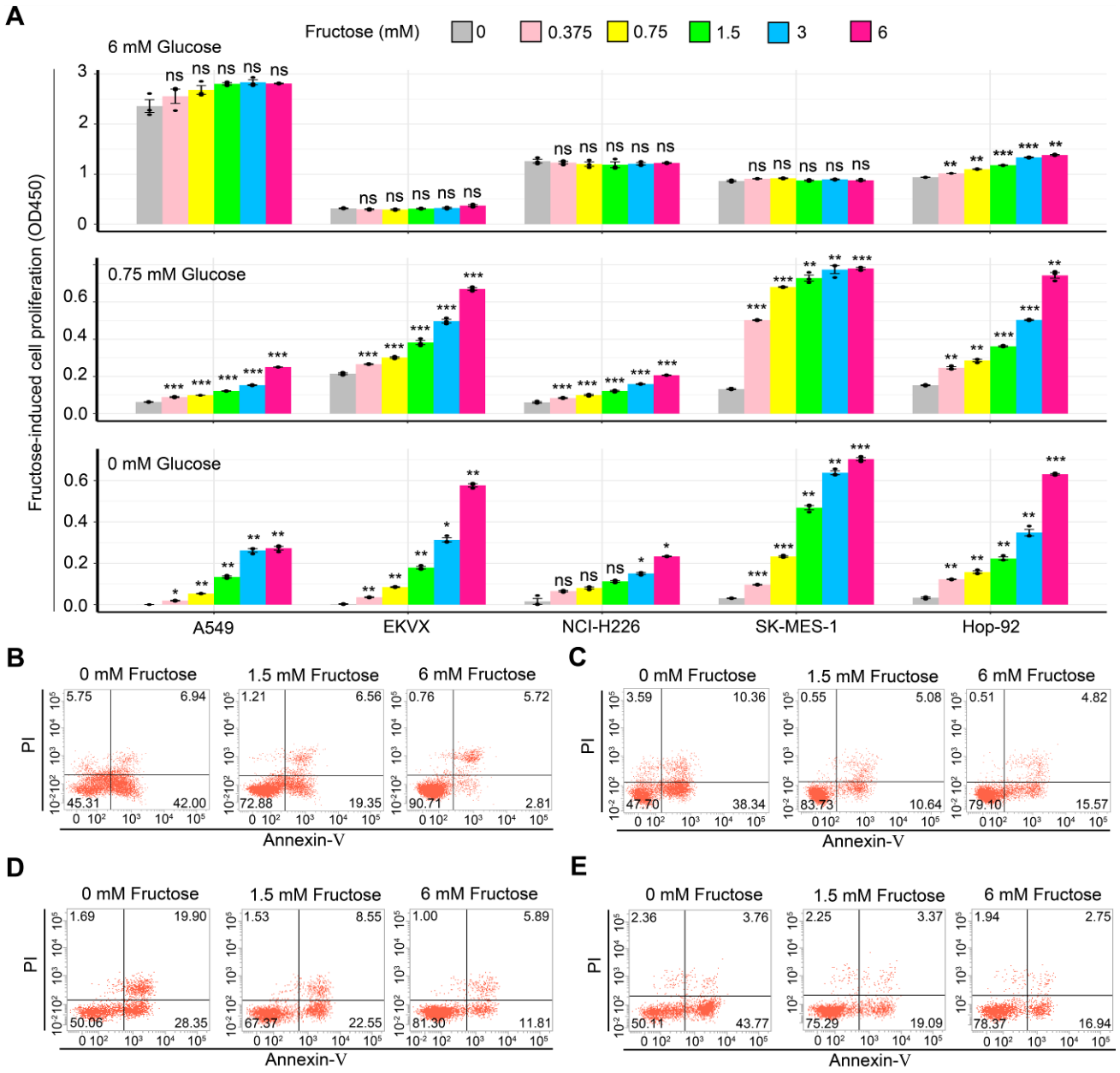

Supplemental Figure 2. Lung cancer cells divert to utilize fructose to promote cell proliferation and cell survival when glucose is deficient or deprived.

(**A**) Fructose-induced lung cancer cell proliferation under conditions of different glucose levels. Cells were cultured in the medium for 72 hours. Statistical analysis was conducted using one-way ANOVA test. For each glucose condition, *P* values were calculated by comparison with the cell proliferation in 0 mM fructose. Under condition of glucose deprivation, due to the unequal variances among subgroups for A549, EKVX, NCI-H226, SK-MES-1 and Hop-92 as shown by the results of homogeneity of variance test, *P* values were acquired from Post Hoc test using Dunnett's T3 algorism. Under condition of 0.75 mM glucose, due to the equal variances among subgroups for A549, EKVX and NCI-H226 as

demonstrated by the results of homogeneity of variance test, *P* values were obtained from Post Hoc test using LSD algorism. Under condition of 0.75 mM glucose, due to the unequal variances among subgroups for SK-MES-1 and Hop-92 as demonstrated by the results of homogeneity of variance test, *P* values were gained from Post Hoc test using Dunnett's T3 algorism. Under condition of 6 mM glucose, due to the unequal variances among subgroups for A549 and Hop-92 as demonstrated by the results of homogeneity of variance test, *P* values were obtained from Post Hoc test using Dunnett's T3 algorism. Under condition of 6 mM glucose, due to the equal variances among subgroups for EKVX, NCI-H226 and SK-MES-1 as demonstrated by the results of homogeneity of variance test, *P* values were obtained from Post Hoc test using LSD algorism. Cumulative data are shown; n = 3. Error bars represent mean ± SEM. $^{*}P < 0.05$, $^{**}P < 0.01$, $^{***}P < 0.001$, 2-tailed test. (**B**-**E**) Cell apoptosis analysis of LC cell lines cultured in medium with no glucose and different concentrations of fructose. A549 (**B**), EKVX (**C**), NCI-H226 (**D**) and Hop-92 (**E**) cells were cultured for 72 hours, 72 hours, 18 hours and 96 hours respectively.

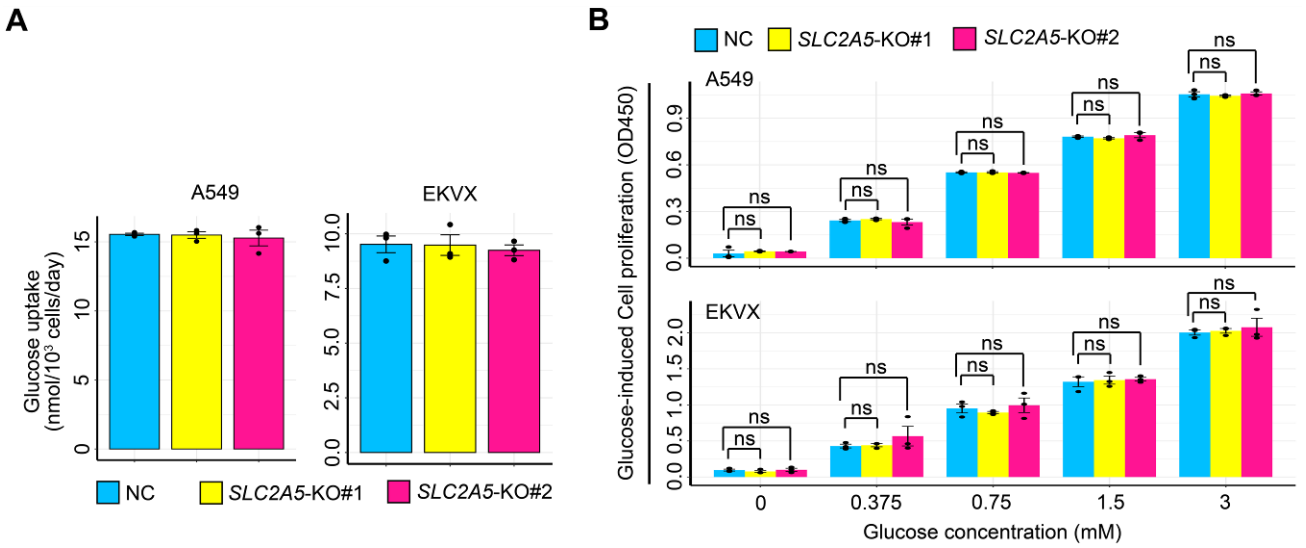

Supplemental Figure 3. *SLC2A5* deletion does not influence glucose uptake and glucose-induced cell growth in lung cells *in vitro*.

(**A**) Glucose uptake by A549 and EKVX cells with or without *SLC2A5* ablation. Cumulative data are shown; n = 3. (**B**) Glucose-induced cell proliferation of A549 and EKVX cells with or without *SLC2A5* ablation. Statistical analysis was conducted using one-way ANOVA test. For A549 cell growth, due to the unequal variances among subgroups for conditions of 0 mM glucose, 0.375 mM glucose and 1.5 mM glucose as demonstrated by the results of homogeneity of variance test, *P* values were gained from Post Hoc test using Dunnett's T3 algorism. Additionally, due to the equal variances among subgroups for conditions of 0.75 mM glucose and 3 mM glucose as demonstrated by the results of homogeneity of variance test, *P* values were gained from Post Hoc test using Dunnett's T3 algorism. For EKVX cell growth, due to the unequal variances among subgroups for conditions of 0.375 mM glucose and 3 mM glucose as demonstrated by the results of homogeneity of variance test, *P* values were gained from Post Hoc test using Dunnett's T3 algorism. In addition, due to the equal variances among subgroups for conditions of 0 mM glucose, 0.75 mM glucose and 1.5 mM glucose as demonstrated by the results of homogeneity of variance test, *P* values were gained from Post Hoc test using Dunnett's T3 algorism. Cumulative data are shown; n = 3. NC, non-target control; KO, knockout. Error bars represent mean ± SEM.

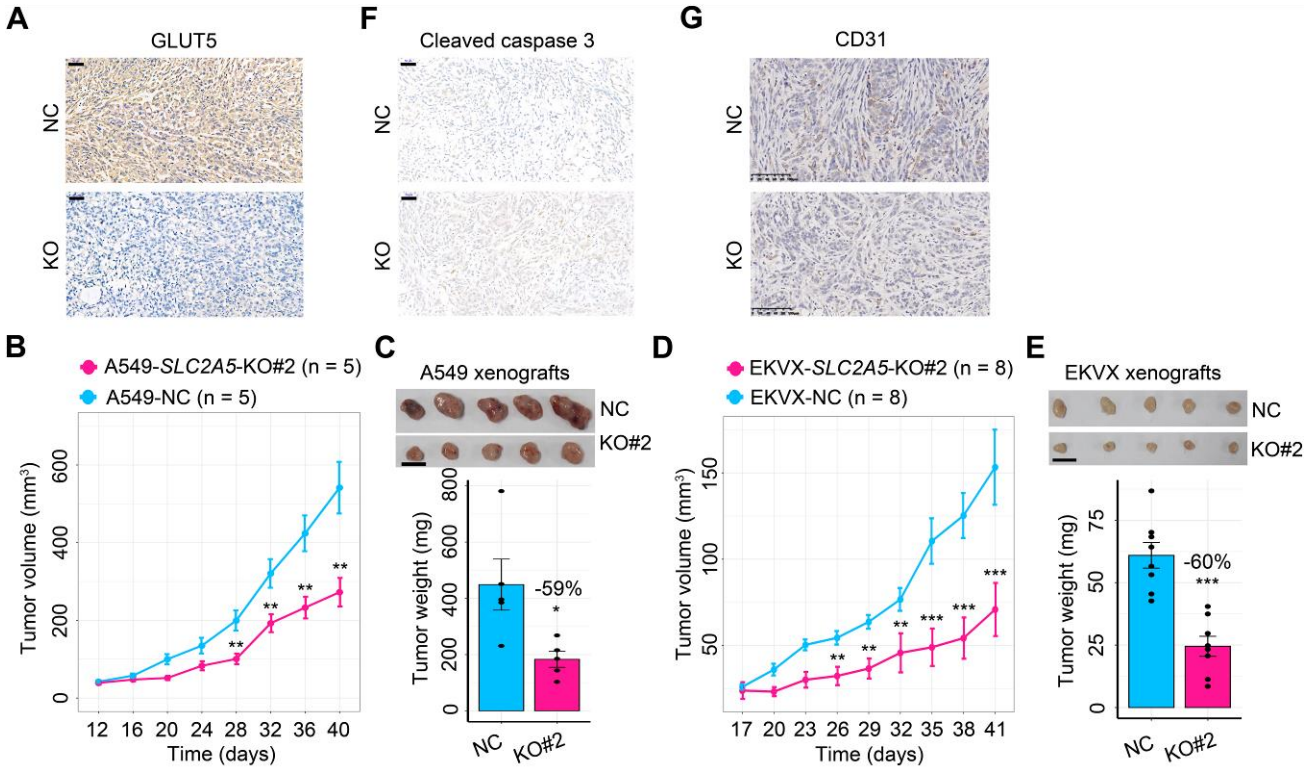

Supplemental Figure 4. The influence of impaired fructose utilization by *SLC2A5* deletion on tumor xenograft growth of lung cancer cells.

(**A**) Immunohistochemistry staining showing GLUT5 expression between control A549 tumor xenografts and A549 tumor xenografts with *SLC2A5* deletion. Scale bar, 50 μm. (**B**) Subcutaneous tumor growth of A549-NC cells and A549- *SLC2A5*-KO#2 cells in nude mice. (**C**) Xenograft tumor images and tumor weight of A549-NC cells and A549- *SLC2A5*-KO#2 cells (n = 5 tumors for each group). Scale bar, 1 cm. (**D**) Subcutaneous tumor growth of EKVX-NC cells and EKVX- *SLC2A5*-KO#2 cells in nude mice. (**E**) Representative xenograft tumor images and tumor weight of EKVX-NC cells and EKVX- *SLC2A5*-KO#2 cells (n = 5 tumors for each group). Scale bar, 1 cm. (**F**) Immunohistochemistry staining revealing cleaved caspase 3 expression between control A549 tumor xenografts and A549 tumor xenografts with *SLC2A5* deletion. Scale bar, 50 μm. (**G**) Immunohistochemistry staining displaying CD31 expression between control A549 tumor xenografts and A549 tumor xenografts with *SLC2A5* deletion. Scale bar, 50 μm.

NC, non-target control; KO, knockout. Error bars represent mean ± SEM. ** $P < 0.01$, *** $P < 0.001$, 2-tailed Student's t test.

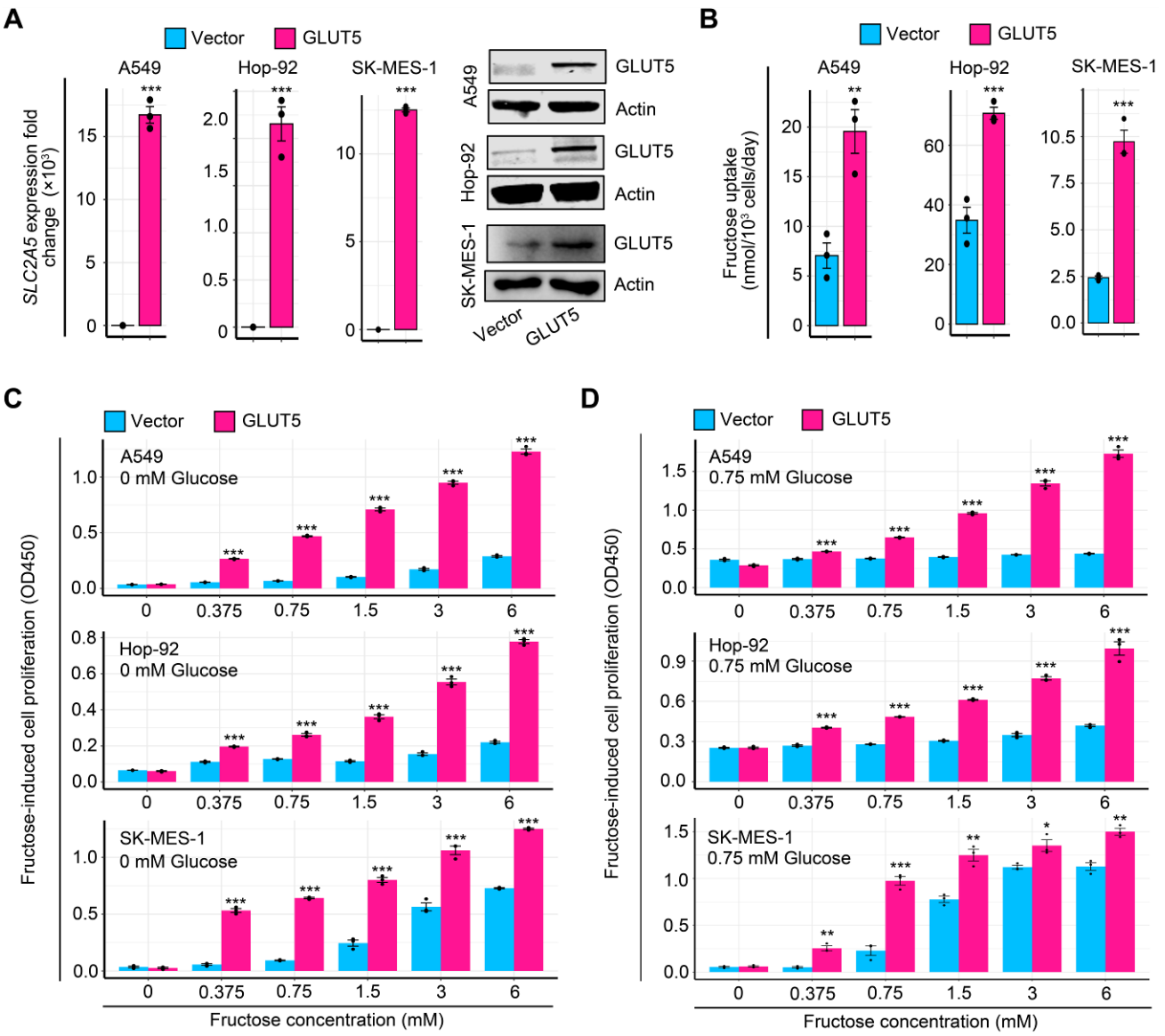

Supplemental Figure 5. Impact of enhanced fructose utilization mediated by enforced GLUT5 expression on fructose uptake and cell proliferation *in vitro*.

(**A**) Measurement of *SLC2A5* and GLUT5 expression in lung cancer cells transfected with the control MigR1 retrovirus or MigR1-GLUT5 retrovirus by q-PCR and Western blot respectively. Cumulative data are shown; n = 3. (**B**) Fructose uptake by lung cancer cells with or without ectopic GLUT5 expression. Cumulative data are shown; n = 3. (**C**) Fructose-induced cell proliferation of lung cancer cells with or without enforced GLUT5 expression under no glucose condition. For each fructose concentration, *P* values were obtained by comparison with the proliferation of cells transfected with control vector. Cumulative data are shown; n = 3. (**D**) Influence of enhanced fructose utilization mediated by ectopic GLUT5 expression on lung cancer cell proliferation under low glucose (0.75 mM)

condition. For each fructose concentration, *P* values were obtained by comparison with the proliferation of cells transfected with control vector. Cumulative data are shown; n = 3. Error bars represent mean ± SEM. $^{*}P < 0.05$, $^{**}P < 0.01$, $^{***}P < 0.001$, 2-tailed Student's t test.

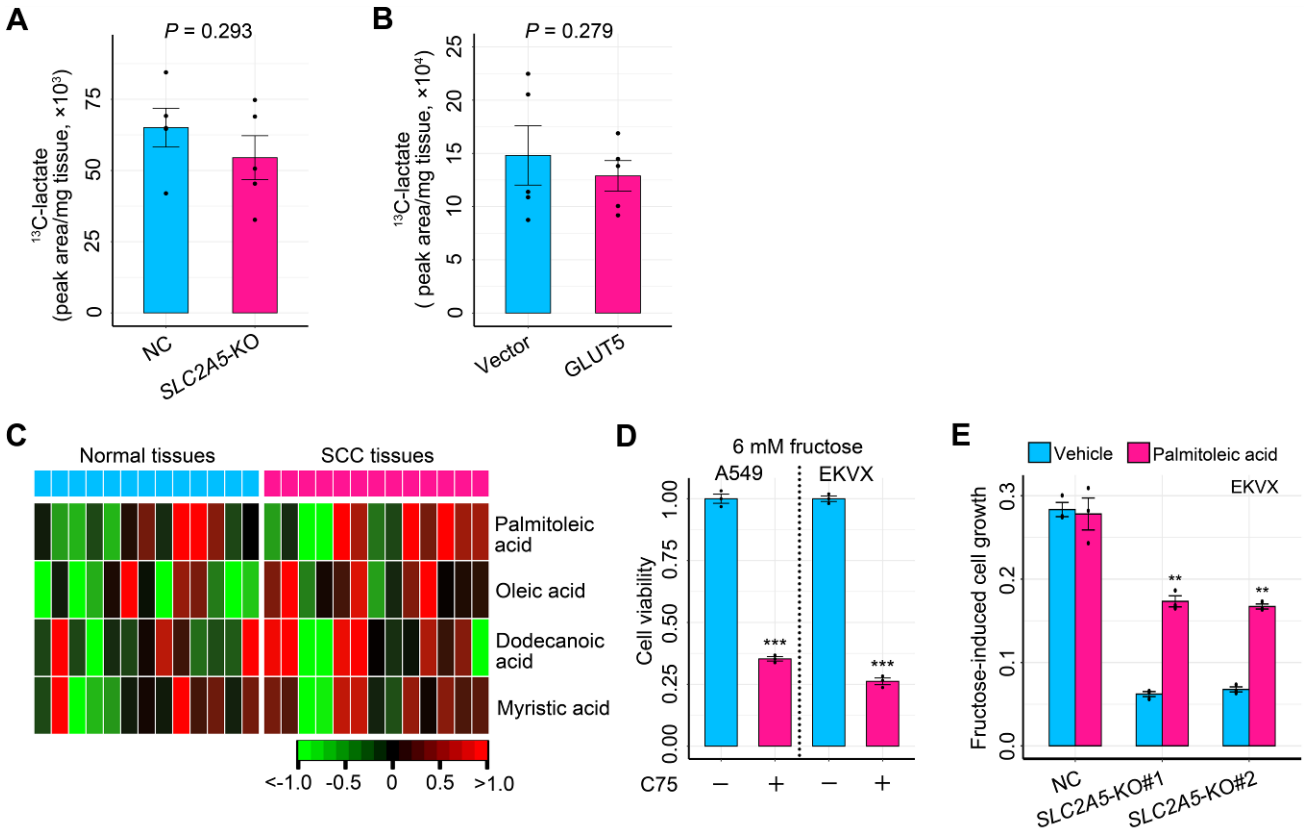

Supplemental Figure 6. Fatty acid concentrations between adjacent normal and tumorous lung tissues of patients with squamous cell carcinoma, and the importance of fatty acid synthesis for fructose-induced lung cancer cell growth.

(**A**) Production of ^{13}C-lactate derived from ^{13}C-fructose in A549 xenografts with or without *SLC2A5* ablation (n = 5 tumors for each group). 2-tailed Student's t test. (**B**) Production of ^{13}C-lactate derived from ^{13}C-fructose in A549 xenografts with or without GLUT5 overexpression (n = 5 tumors for each group). 2-tailed Student's t test. (**C**) Heatmap showing fatty acid concentrations between adjacent normal and tumorous lung tissues of patients with squamous cell carcinoma (n = 13). (**D**) Impact of the FASN inhibitor C75 on fructose-induced cell growth of A549 and EKVX. Cells were grown in the medium containing 6 mM fructose with or without C75 (100 μM). Cumulative data are shown; n = 3. (**E**) Palmitoleic acid supplement restored the *in vitro* growth of EKVX cells with *SLC2A5* ablation. Cells were cultured in complete medium containing 6mM fructose for 72 hours. The concentration for palmitoleic acid was 50 μM. Cumulative data are shown; n = 3.

NC, non-target control; KO, knockout. Error bars represent mean ± SEM. $^{**}P < 0.01$, $^{***}P < 0.001$, 2-tailed Student's t test.

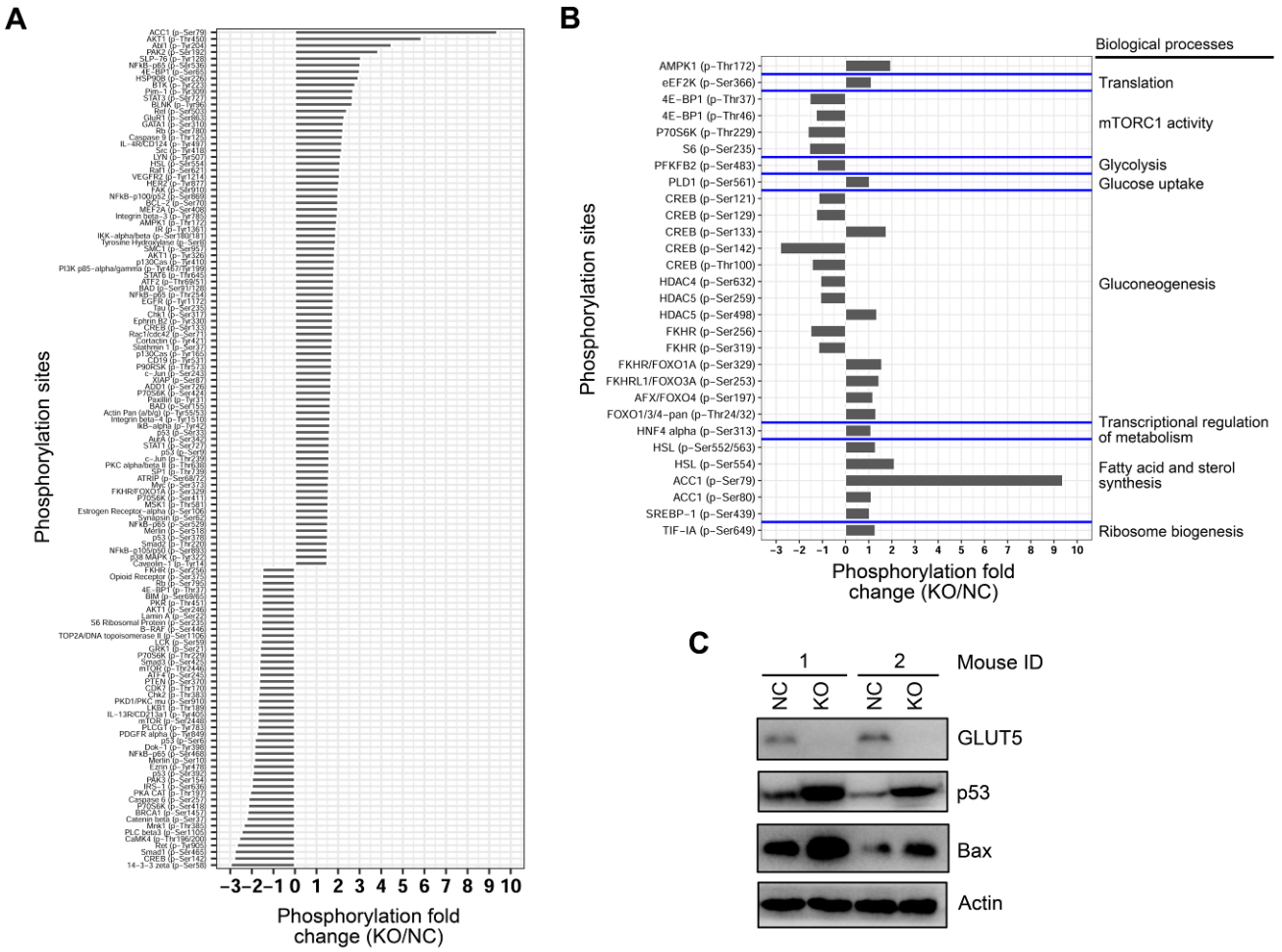

Supplemental Figure 7. Phospho-protein profiling between A549 tumor xenografts with *SLC2A5* deletion and those without *SLC2A5* deletion.

(**A**) Phospho-proteomics assay of A549 tumor xenografts with or without *SLC2A5* ablation. Proteins with phosphorylation levels increased by 50% or decreased by 50% in A549-*SLC2A5*-KO tumor xenografts relative to A549-NC tumor xenografts were presented. (**B**) Phosphorylation alteration of downstream targets of AMPK in A549-*SLC2A5*-KO tumor xenografts relative to A549-NC tumor xenografts. (**C**) Western blot showing the expression of p53 and Bax between A549 tumor xenografts with *SLC2A5* deletion and control A549 tumor xenografts.

NC, non-target control; KO, knockout.

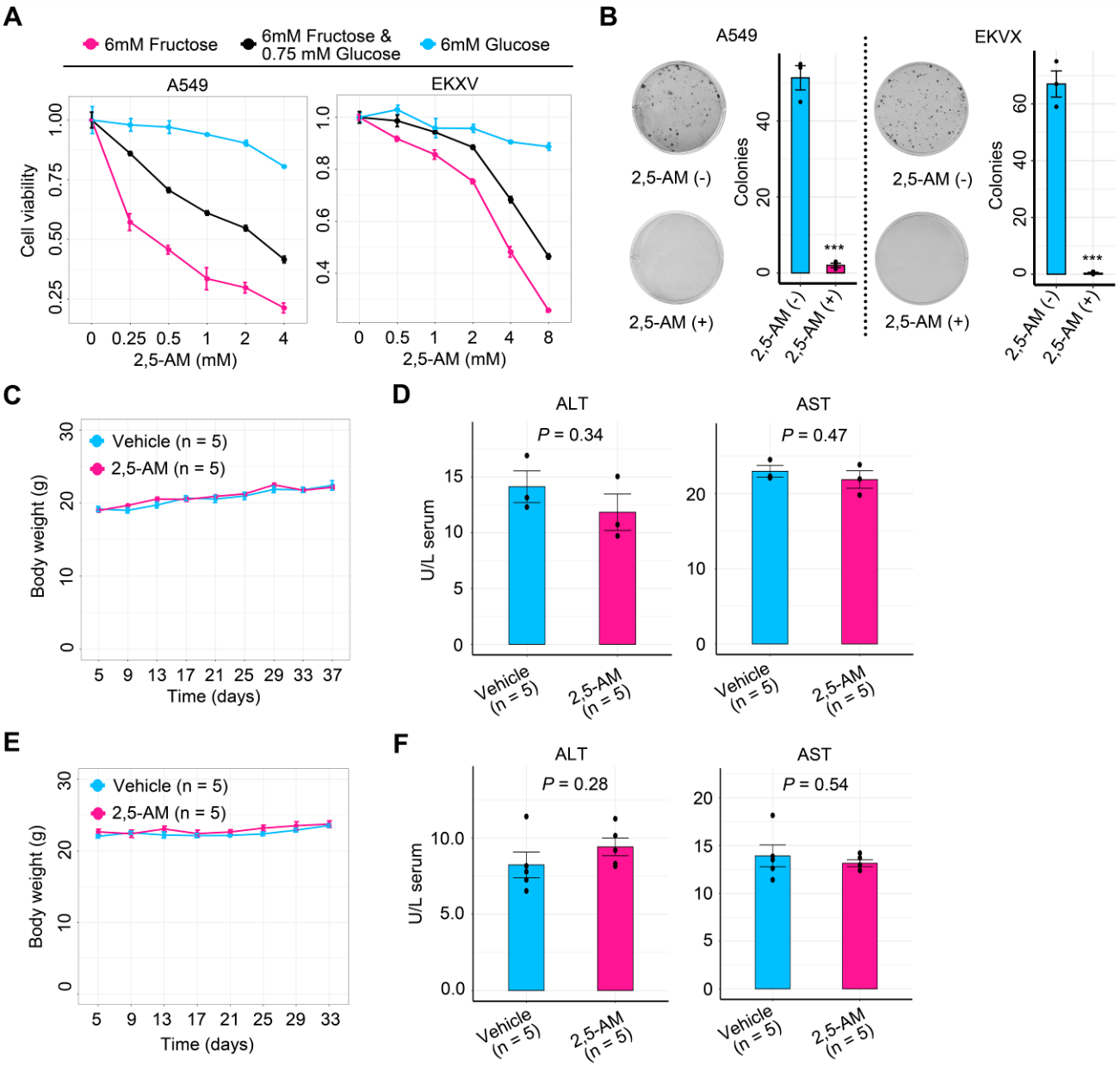

Supplemental Figure 8. Pharmacological treatment using a GLUT5 inhibitor, 2,5-anhydro-D-mannitol (2,5-AM), restrains the neoplastic growth of lung cancer and exhibits negligible side effects.

(**A**) Proliferation of lung cancer cells treated with 2,5-AM under distinct carbon source conditions. Cumulative data are shown; n = 3. (**B**) Colony growth of A549 and EKVX cells in medium containing 6 mM fructose with or without 2,5-AM (4 mM) treatment. Cumulative data are shown; n = 3. (**C**) Body weight curve of mice bearing A549 tumors treated with vehicle or 2,5-AM. (**D**) Blood alanine transaminase (ALT) and aspartate transaminase (AST) levels in mice bearing A549 tumors treated with vehicle or 2,5-AM (n = 5 for each group). (**E**) Body weight curve of mice bearing EKVX tumors treated with vehicle or 2,5-AM. (**F**) Blood ALT

and AST levels in mice bearing EKVX tumors treated with vehicle or 2,5-AM (n = 5 for each group).

Error bars represent mean ± SEM. *P* values were computed using 2-tailed Student's t test. *** $P < 0.001$.

Supplemental Table 1. Key resources table

REAGENT or RESOURCE	SOURCE	IDENTIFIER
Chemicals, Peptides, and Recombinant Proteins		
[U-^{13}C6] -D-fructose	Cambridge Isotope Laboratories	CLM-1553-1
2,5-Anhydro-D-mannitol	TRC	649000
Lipofectamine 3000	Thermo Fisher Scientific	L3000008
Hexadimithrine bromide	Sigma	H9268-5G
D-Fructose	Sigma	P3510-500G
D-Glucose	Sigma	G7012-1KG
Palmitoleic acid	Sigma	P9417
Bovine serum albumin	Equitech-Bio	BAH66-0050
Oligonucleotides		
CRISPR guide RNA for non-target (NT) control: FWD: AAGAAGAATTGGGGATGATG REV: CATCATCCCCAATTCTTCTT	Addgene	N/A
CRISPR guide RNA #1 for human *SLC2A5*: FWD: CCCAGCCGCGCAGCGTCTGT REV: ACAGACGCTGCGCGGCTGGG	Addgene	N/A
CRISPR guide RNA #2 for human *SLC2A5*: FWD: CCCAGGCTGGCCGATCCTGC REV: GCAGGATCGGCCAGCCTGGG	Addgene	N/A
CRISPR guide RNA #1 for human *FASN*: FWD: CGACCCACCTCCGTCCACGA REV: CGACCCACCTCCGTCCACGA	Addgene	N/A
CRISPR guide RNA #2 for human *FASN*: FWD: TACGCCACCATCCTGAACGC REV: GCGTTCAGGATGGTGGCGTA	Addgene	N/A
CRISPR guide RNA #1 for Human *HIF1A*: FWD: CCTCACACGCAAATAGCTGA REV: TCAGCTATTTGCGTGTGAGG	Addgene	N/A
CRISPR guide RNA #2 for Human *HIF1A*: FWD: TGTTTACAGTTTGAACTAAC REV: GTTAGTTCAAACTGTAAACA	Addgene	N/A
Primers for full-length human *SLC2A5*: FWD: CATGCCATGGAGCAACAGGATCAGAGC REV: CATGCCATGGACTGTTCCGAAGTGACAGG	This study	N/A
Primers for q-PCR, see Supplemental table 3	This study	N/A
Critical Commercial Assays		
FITC Annexin V Apoptosis Detection Kit I (RUO)	BD	556547
Cell Counting Kit-8(CCK-8)	Dojindo	CK04
High Sensitivity Fructose Assay Kit	Sigma	MAK180-1KT

Glucose (HK) Assay Kit	Sigma	GAHK20-1KT
SYBR® Premix Ex Taq™ (Tli RNase H Plus)	Takara	RR42WR
Alanine aminotransferase Assay Kit	Nanjing Jiancheng Bioengineering Institute	C009-2
Aspartate aminotransferase Assay Kit	Nanjing Jiancheng Bioengineering Institute	C010-2
Experimental Models: Cell Lines		
A549	NCI	N/A
Hop-92	NCI	N/A
EKVX	NCI	N/A
NCI-H226	NCI	N/A
SK-MES-1	Stem Cell Bank, Chinese Academy of Sciences	SCSP-5010
293T	ATCC	CRL-3216
Experimental Models: Organisms/Strains		
Mouse: BALB/c-nude	Shanghai SLAC Laboratory Animal Co.,Ltd	N/A
Recombinant DNA		
MigR1 vector	Addgene	27490
MigR1-human GLUT5 vector	This study	N/A
VSVG packaging vector	Addgene	14888
Gag/pol packaging vector	Addgene	14887
Lenti-cas9-BSD vector	Addgene	52962
psPAX2 packaging vector	Addgene	12260
pMD2.G packaging vector	Addgene	12259
Lenti-Guide-puro-guide RNA for NT control	Addgene	N/A
Lenti-Guide-puro-guide RNA #1 for human GLUT5	Addgene	N/A
Lenti-Guide-puro-guide RNA #2 for human GLUT5	Addgene	N/A
Lenti-Guide-puro-guide RNA #1 for human FASN	Addgene	N/A
Lenti-Guide-puro-guide RNA #2 for human FASN	Addgene	N/A
Software and Algorithms		
R language	Open source	https://www.r-project.org/
ImageJ software	Open source	https://imagej.nih.gov/ij/
CRISPR Guide RNA database		
Others		
Dialyzed, fetal bovine serum	Thermo Fisher Scientific	26400044
DMEM, no Glucose	Thermo Fisher Scientific	11966025

1

Supplemental Table 2. Mouse diet formula.

Ingredient	Weight (g)
Casein, 30 Mesh	200
L-Cystine	3
Corn Starch	397
Maltodextrin	132
Sucrose	100
Cellulose	50
Soybean Oil	70
t-Butylhydroquinone	0.014
Mineral Mix S10022G	35
Vitamin Mix V10037	10
Choline Bitartrate	2.5
Total	1000

Supplemental Table 3. Primer sequence for q-PCR.

Gene	Species	NCBI Locus ID	Forward primer sequence (5'→3')	Reverse primer sequence (5'→3')
SLC2A5	Human	NM_003039	TCTGTAACCGTGTCCATGTTTC	CATTAAGATCGCAGGCACGATA
ACTIN	Human	NM_001101.3	CACTCTTCCAGCCTTCCTTC	GTACAGGTCTTTGCGGATGT

Figure2E

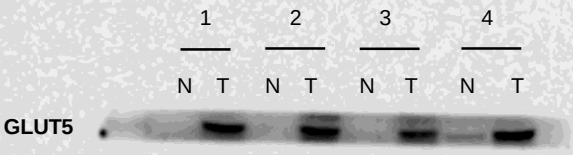

Figure2E

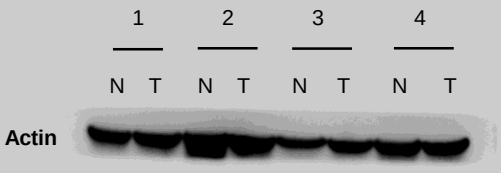

Figure2F

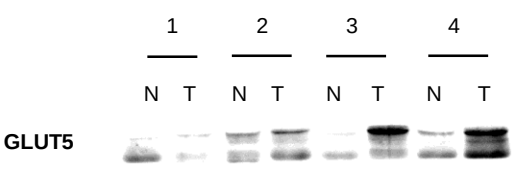

Figure2F

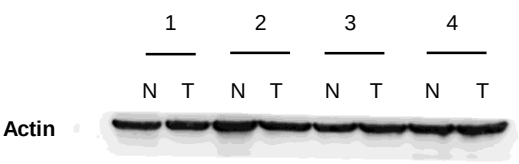

Figure4A

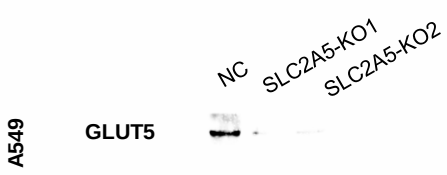

Figure4A

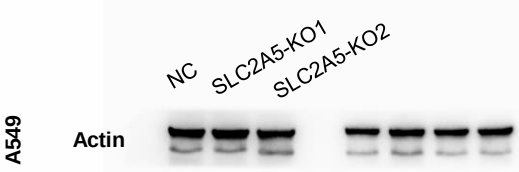

Figure4A

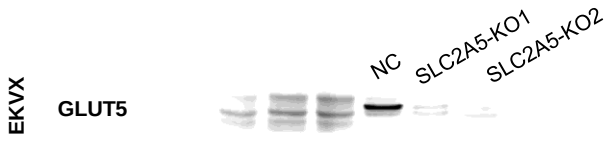

Figure4A

Figure5A

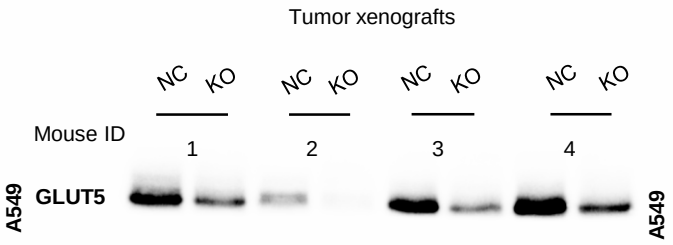

Figure5A

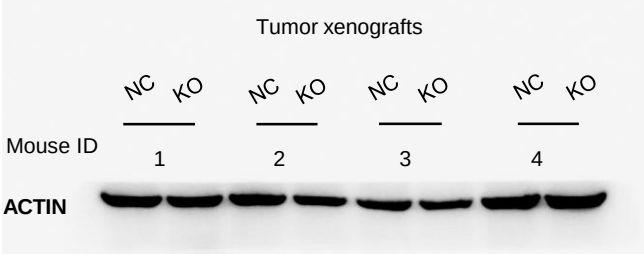

Figure5A

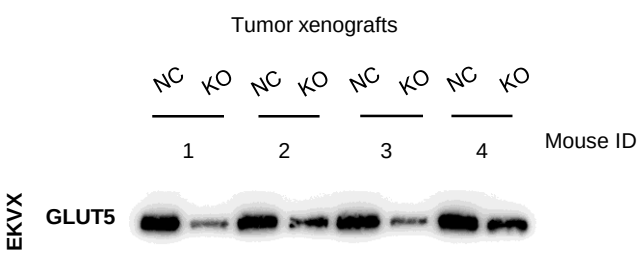

Figure5A

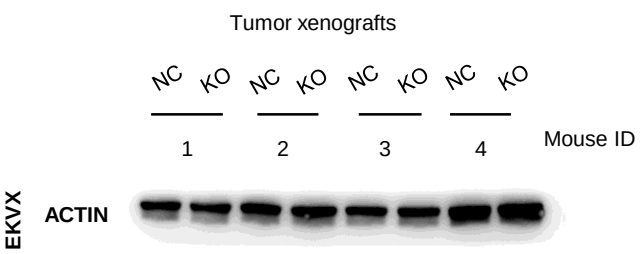

Figure5G

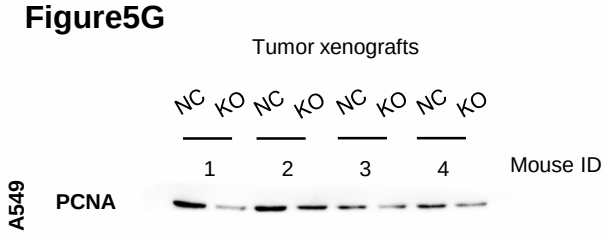

Figure5G

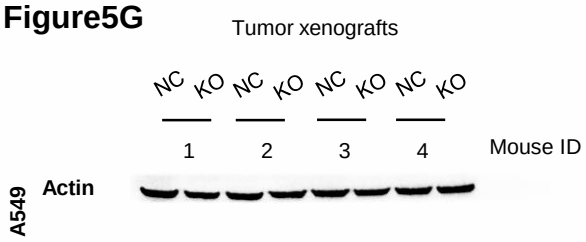

Figure5G

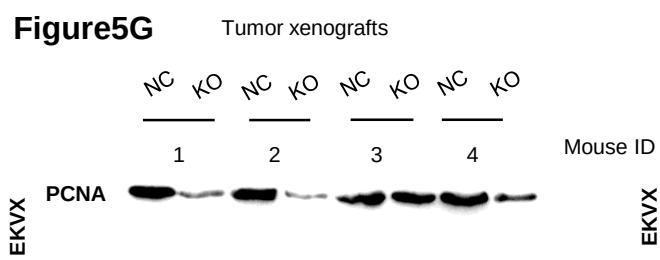

Figure5G

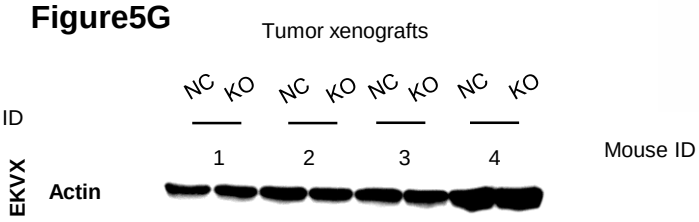

Figure6A

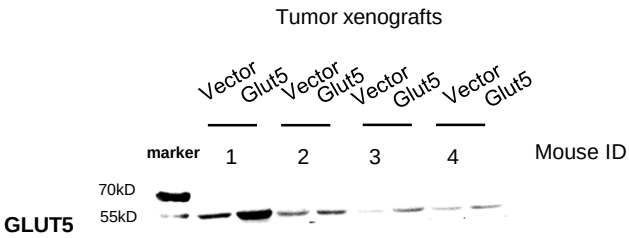

Figure6A

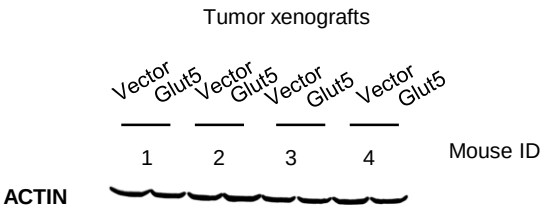

Figure6E

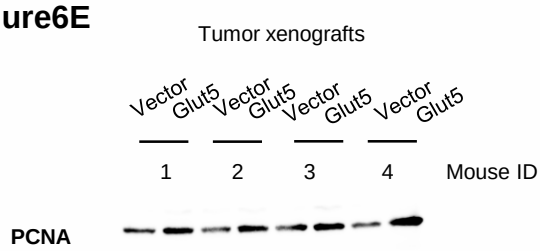

Figure6E

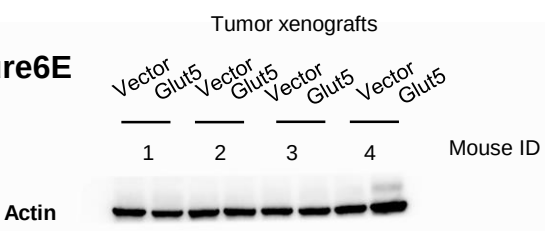

Figure8A

Figure8A

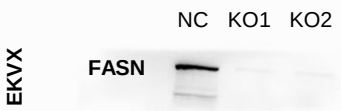

Figure8A

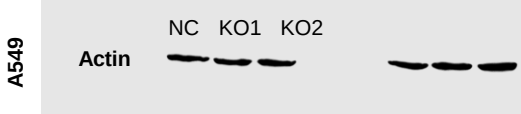

Figure8A

Figure9B

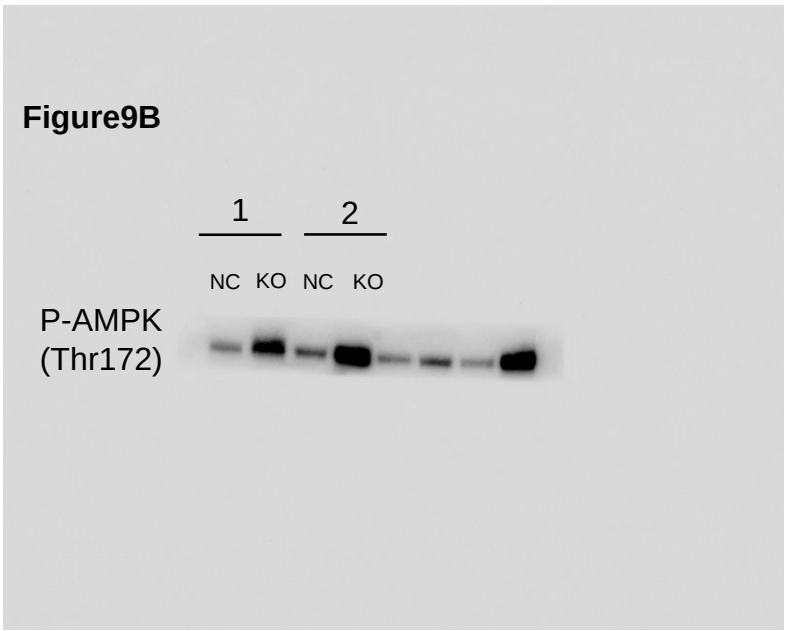

Figure9B

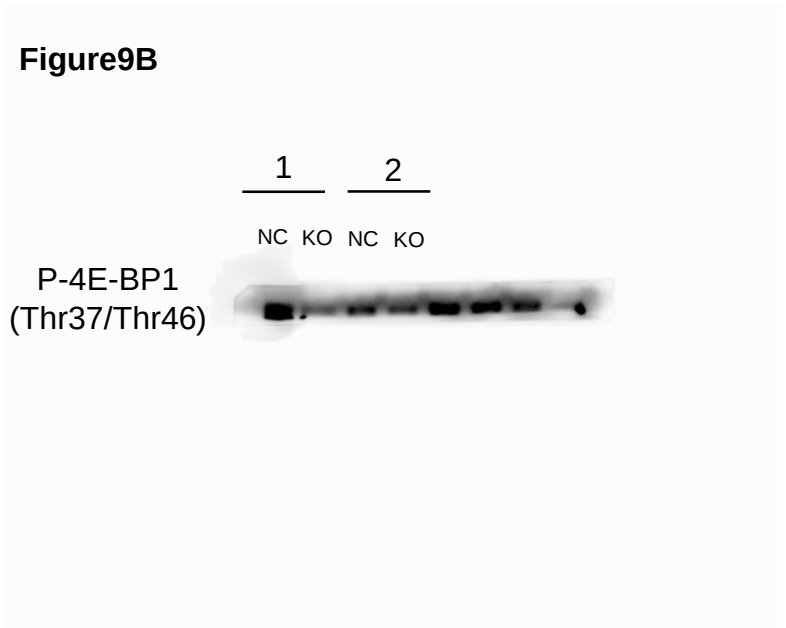

Figure9B

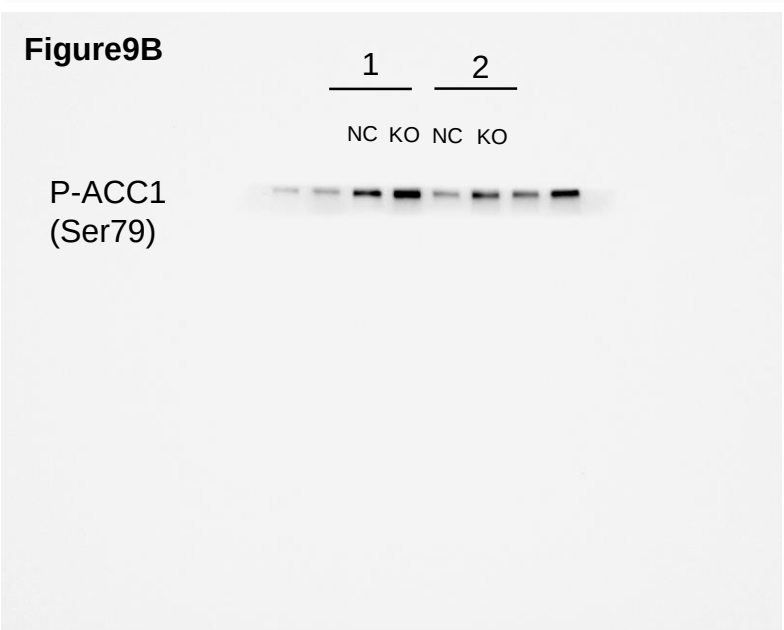

Figure9B

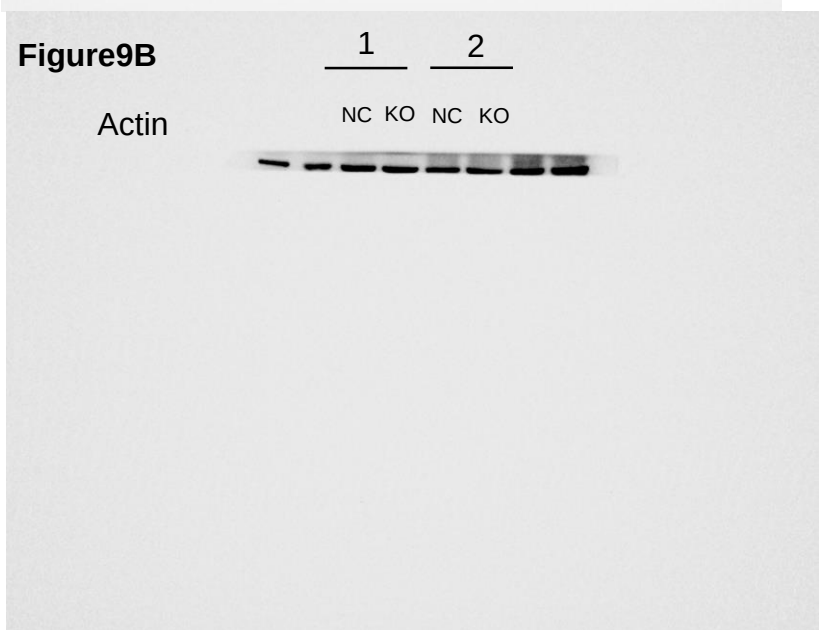

Figure9D

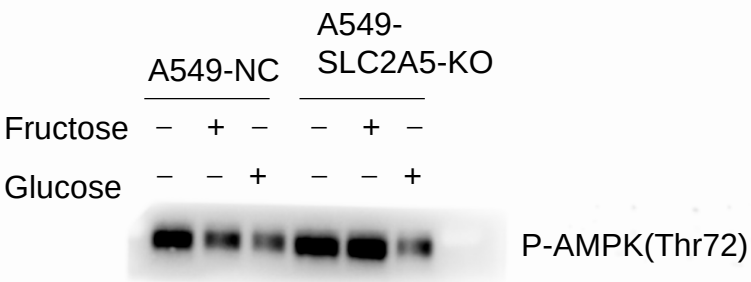

Figure9D

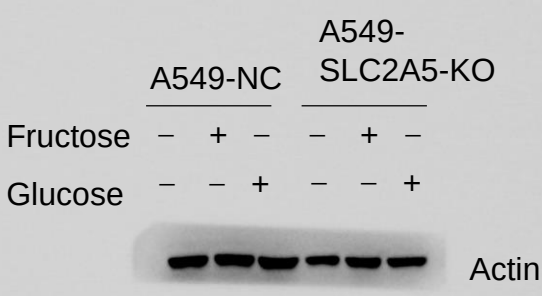

Figure9E

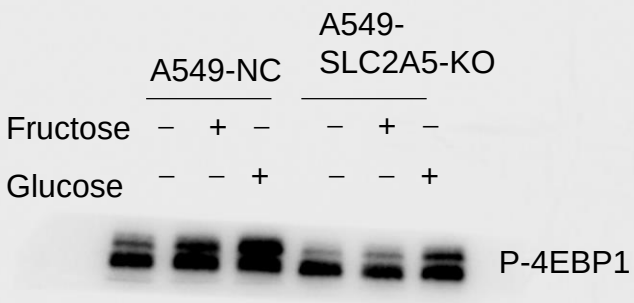

Figure9E

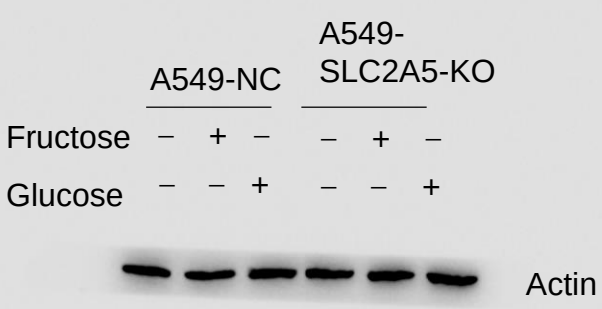

Figure9F

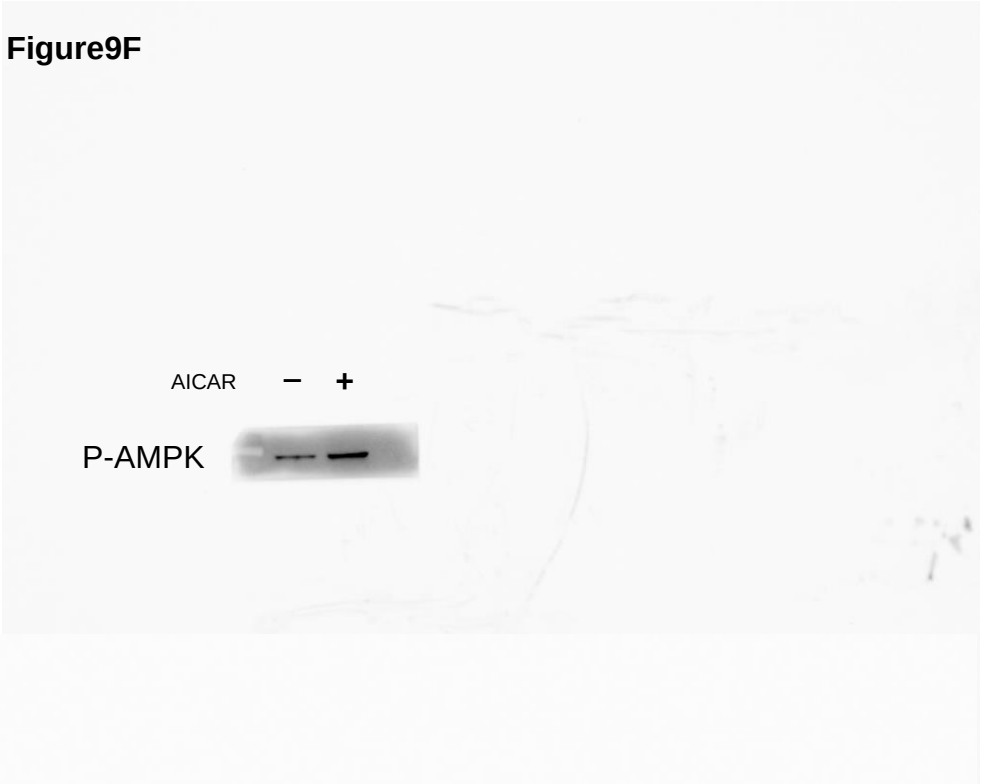

Figure9F

Figure9F

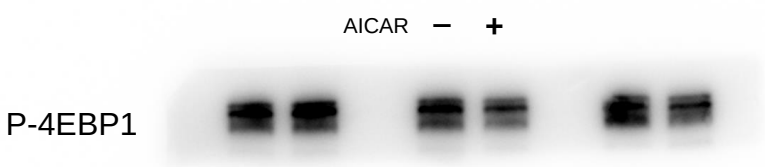

Figure9F

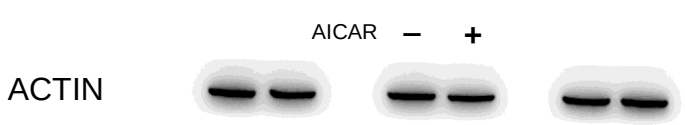

Supplemental Figure 5A

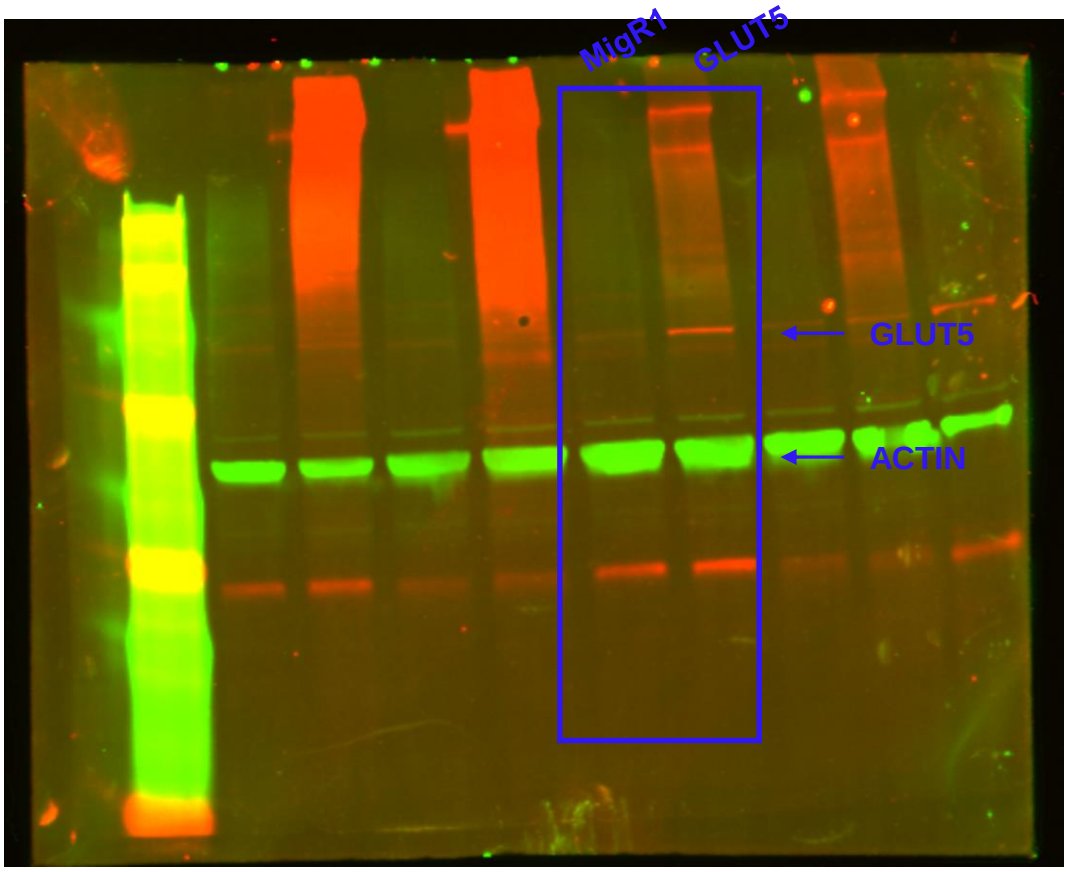

Supplemental Figure 5A

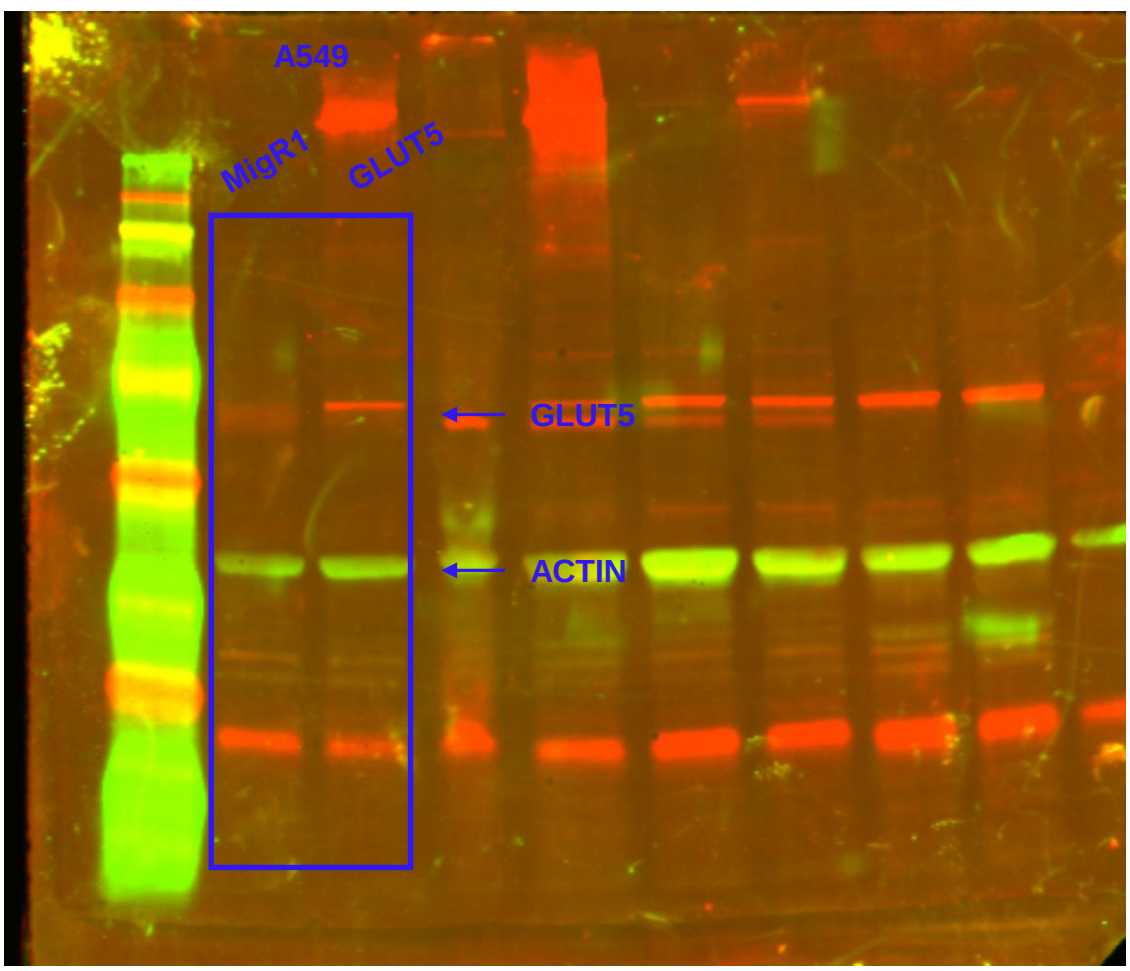

Supplemental Figure 5A

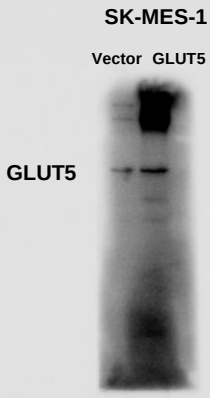

Supplemental Figure 5A

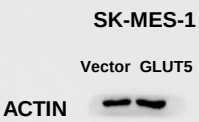

Supplemental Figure 7C

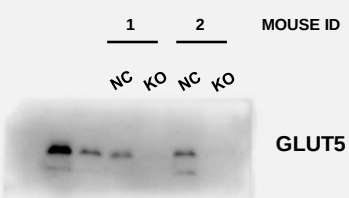

Supplemental Figure 7C

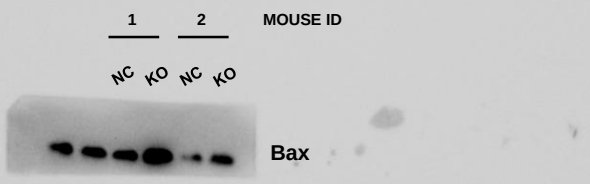

Supplemental Figure 7C

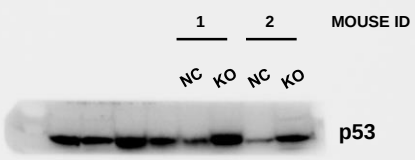

Supplemental Figure 7C